processes

MDPI

Article

Tailored Polylactic Acid/Polycaprolactone Blends with Excellent Strength–Stiffness and Shape Memory Capacities

Todor Batakliev *, Vladimir Georgiev, Evgeni Ivanov, Verislav Angelov and Rumiana Kotsilkova

Open Laboratory on Experimental Micro and Nano Mechanics (OLEM), Institute of Mechanics, Bulgarian Academy of Sciences, Acad. G. Bonchev Str. Block 4, 1113 Sofia, Bulgaria; vgeorgiev@imbm.bas.bg (V.G.); ivanov_evgeni@imbm.bas.bg (E.I.); v.angelov@imbm.bas.bg (V.A.); kotsilkova@imbm.bas.bg (R.K.)

* Correspondence: batakliev@imbm.bas.bg

Abstract: The present work deals with the mixing of two green polymers at several definite ratios that led to the receiving of biodegradable polylactic acid (PLA)/polycaprolactone (PCL) blends possessing well-expressed macromechanical and shape memory properties. Four non-compatibilized polymer compositions were prepared by using a twin-screw melt extrusion technique, allowing for a homogeneous dispersion of the PCL droplets in the PLA matrix and higher interfacial adhesion between the two phases. The mechanical behavior of the specimens was estimated by tensile experiments conducted at three particular crosshead velocities. It was established that the addition of PCL as a soft segment redounded to an increment of the toughness and elongation at ultimate strength of the polymer composite at the expense of the maximum tensile stress and Young's modulus. These latter two parameters were found to be more sensitive, in terms of reaching high values, to the content of PLA as a hard segment in the polymer blend. Performing thermoresponsive shape memory tests disclosed an overwhelming reversibility between the temporary and permanent states of the composite materials, including significant shape fixation (R_f) and shape recovery (R_r) rates. SEM analysis of the PLA/PCL compositions revealed a distinct phase-separated microstructure, confirming the immiscibility of the two polymers in the blend.

Keywords: green polymer blends; tensile testing; shape memory effect; phase separation; composite microstructure

check for updates

Academic Editors: Anil K. Bhowmick and Lee Tin Sin

Received: 28 February 2025
Revised: 15 April 2025
Accepted: 23 April 2025
Published: 26 April 2025

Citation: Batakliev, T.; Georgiev, V.; Ivanov, E.; Angelov, V.; Kotsilkova, R. Tailored Polylactic Acid/Polycaprolactone Blends with Excellent Strength–Stiffness and Shape Memory Capacities. *Processes* **2025**, *13*, 1328. https://doi.org/10.3390/pr13051328

Copyright: © 2025 by the authors. Licensee MDPI, Basel, Switzerland. This article is an open access article distributed under the terms and conditions of the Creative Commons Attribution (CC BY) license (https://creativecommons.org/licenses/by/4.0/).

1. Introduction

Over the last several years, biodegradable polymers, such as polylactic acid (PLA) and polycaprolactone (PCL), have greatly attracted the attention of the scientific community in the process of the development of new green composite materials [1–4] intended for a wide range of useful applications [5–8]. The combination of shape memory effect (SME) and good mechanical properties is always needed when searching for a reliable polymer blend consisting of a mobile soft phase and an elastic hard phase. The balance between some mechanical parameters, such as Young's modulus, tensile strength, and elongation up to the fracture point, can play an important role in the selection of a polymer composition possessing shape memory function [9]. Another mechanical feature that is likely to be modified by the presence of polycaprolactone in a mixture with polylactic acid is the toughness of as-prepared composite material [10]. Increasing the amount of energy absorbed per unit volume up to the point of break in the course of the stretching process is an effective way to overcome the brittleness, as one of the main shortcomings of the PLA matrix, with paltry reduction in its stiffness. The size distribution of the soft polymer's

particles has a sensitive impact on the toughness of a PLA/PCL blend, as well as on the ratio between the contents of both components, even in the absence of a compatibilizer [11]. A study on the morphology and mechanical properties of PLA/PCL composites prepared by melt extrusion showed a dependence of the maximum elongation of the polymer blend on the fine dispersion of the PCL particles and the degree of crystallinity of the PLA die [12]. It has been reported that being part of such polymer composition, PCL can behave as a polymeric plasticizer, reducing the elastic modulus and the yield stress but improving the flexibility and the ductility of the blend [13]. Tensile testing has often been described in research articles as a proper method for the mechanical characterization of PLA/PCL materials [2,14], though in most cases, a single crosshead velocity was applied, which may constrain the careful analysis of the polymer composites' elastic–plastic behavior. In the light of receiving biodegradable PLA/PCL blends with thermally induced shape memory behavior, it should be pointed out the influence of the composition ratio and crystallinity of the separate polymer phases [15,16]. A relatively good shape fixation rate (R_f) of 95.80% and a shape recovery rate (R_r) of 67.62% have been calculated for a hot-pressed sample consisting of PLA and PCL particles with a weight percent ratio of 80/20 [17]. Exploring melt-extruded PLA/PCL blends with PCL content varying in the range of 10–60 wt% has uncovered the mutual influence of the crystallinity of the reversible PCL domain and the glass transition behavior of the fixed PLA domain on the specimens' shape memory performance [18]. Temperature-induced shape memory testing, studied by spiral bending [9] and circulating volume elongational strain [16], evidenced shape recovery ratios of 89% and 94%, respectively, for a 70/30 w/w% PLA/PCL blend. In both investigations, a dependence of the polymer compositions' shape recovery and shape fixing behavior on the content of PLA was reported. In another paper, it has been claimed that a 30% mass fraction of PLA in a PLA/PCL composite gives the best shape recovery rate of 76%, which was explained by a more beneficial continuous phase microstructure and favorable compatibility at a 30/70 wt% ratio between the two polymer phases [19].

The goal of the present study was to conduct a thorough mechanical characterization of a series of PLA/PCL composite blends by applying different crosshead velocities in the script of the tensile testing mode. Based on this approach, the complex elastic–plastic behavior of the dual-phase polymer compositions that would contribute to the searching of samples with tuned mechanical properties was ascertained. Only such kind of polymer blends should be selected for the study of SME controlled by main factors as the elastic modulus of the hard phase and the movement of the soft phase. The novelty of the current research work is emphasized by the sophisticated macromechanical investigation, amplified by the process of tailoring a range of new biodegradable polymer samples with an appropriately designed microstructure and great shape memory performance.

2. Materials and Methods

2.1. Materials

Polylactic acid (PLA) with formulated grade Ingeo™ 3D850, possessing a melt mass-flow rate of 9–15 g/10 min (210 °C/2.16 kg), was purchased from Nature Works (Plymouth, MN, USA). The second biopolymer material, polycaprolactone (PCL), having a molecular weight M_n of 70,000–90,000 g/mol and an MFI 2–4 g/10 min (160 °C/5.00 kg), was bought from Sigma Aldrich (St. Louis, MI, USA). Both output biopolymers were received in the shape of pellets. The degrees of crystallinity of the neat PLA and PCL, found to be 14.3% and 42.6% respectively, were calculated by DSC measurements reported in a recent article [20].

2.2. Preparation of PLA/PCL Composite Polymer Blends

Before processing, the PLA and PCL pellets were meticulously dried in a vacuum oven for optimal material quality. The PLA was dried at 80 °C for six hours, while the PCL was dried at 40 °C for an equal length of time.

Subsequently, the dried polymers were precisely weighed and combined in four distinct ratios (PLA wt%/PCL wt%): 95/5, 70/30, 60/40, and 30/70. Each mixture was then thoroughly homogenized by manual blending within sealed zip-lock bags to ensure a uniform dispersion of the components.

The resulting blends were subsequently processed using a Process 11 (Thermo Scientific, Waltham, MA, USA) co-rotating twin-screw extruder. The extruder's temperature profile was optimized, with the first two zones set at 175 °C, the third at 180 °C, and zones four to seven maintained at 190 °C. The die temperature was set at 180 °C, with a screw rotating speed of 150 rpm. The screw torque during extrusion was maintained within 60–70%.

Upon extrusion, the polymer filament was subjected to a controlled cooling process. Two water baths, maintained at 65 °C and 25 °C respectively, were employed to gradually cool the extrudate. This controlled cooling regimen facilitated the solidification of four distinct PLA/PCL composite materials in the form of filaments with a diameter of 1.75 ± 0.5 mm, each with a unique composition, as denoted in Table 1.

Table 1. List of melt-extruded PLA/PCL compositions.

Polymer Blend	PLA, wt%	PCL, wt%
95PLA/5PCL	95	5
70PLA/30PCL	70	30
60PLA/40PCL	60	40
30PLA/70PCL	30	70

2.3. Elaboration of Test Samples

The extruded filaments were converted into dog-bone samples for tensile testing by hot-pressing the pelletized polymer material in a metallic mold at 180 °C, using a hydraulic press with heating plates (Carver, Wabash, IN, USA). Undesired adhesion and material waste were avoided by placing the mold between two Teflon® sheets. The size of the working section, that is, the narrow portion of each dog-bone specimen, subjected to tensile stress, was fixed at 10 mm as a requirement of the experimental setup. The standard thickness and width of the dog bone's narrow portion had dimensions of ~1 mm and ~2.5 mm, respectively. Every deviation from these sizes was taken into account when calculating the main mechanical parameters of the samples. Hot-pressed composite strips with a thickness of ~1 mm were used for the shape memory tests. SEM analysis was performed on the cross-sectional surface of polymer filaments, which were cut in advance under liquid nitrogen and coated with a gold nanolayer in order to make the samples conductive.

2.4. Shape Memory Experiments

Hot-pressed polymer films from extruded filaments were cut into rectangular strips with dimensions of $60 \times 10 \times 1$ mm. The sheer shape memory experiments on the series of composite blends were conducted in bending mode using a simple homemade device. After snapping the initial permanent shape of the thermally responsive specimens, each one of them was subjected to a deformation thoroughly measured during a heating–cooling process consisting of the following steps:

1. Sinking the strip for 10 s in a water bath already heated to 60 °C to ensure a uniform sample warming. This temperature was not randomly selected, as the glass transition (T_g) of PLA and the melting temperature of PCL (T_m) were defined by DSC analysis to be 59.7 °C and 63.8 °C, respectively [21]. Standing immersed in the hot water, the sample was bent to an angle of 180° by means of a metallic brace.
2. Keeping the applied force unchanged, the sample was transferred to cold water at 5 °C, where it was held for 10 s. After cooling, the external load was withdrawn in order to ascertain the temporary shape of the polymer strip and to record the bending angle of fixation as θ_1.
3. In the third step, after leaving it to rest for 20 min at room temperature, the specimen was placed again in a warm water bath at 60 °C to recover its permanent state. Then, the strip was pulled off the bath, and the bending angle of recovery was measured and written down as θ_2.
4. Both bending angles θ_1 and θ_2, which were needed to calculate R_f and R_r, were measured using ImageJ software (version 1.54k).

The shape fixation rate (R_f) and shape recovery rate (R_r) of the polymer blends were calculated by the following equations:

$$R_f = \frac{\theta_1}{180} \times 100\% \quad (1)$$

$$R_r = \frac{\theta_1 - \theta_2}{\theta_1} \times 100\% \quad (2)$$

2.5. Instrumental Methods

Tensile experiments were carried out on UMT-2 Universal Tester modular system (Billerica, MA, USA) developed by Bruker. The tests were conducted using a 1–100 kg (1000 N) force sensor at room temperature. For better comprehending of the mechanical behavior of the polymer blends, three work velocities of 1, 5, and 10 mm/min were applied. The standard error of the measured parameters was determined by testing 5 dog-bone samples for each polymer composition. Prior to get the mechanical data by plotting the experimental stress–strain curves, the accurate values of thickness and width of the work section of each specimen were inserted into the instrumental software.

The morphology of the fractured cross-section polymer blend surface was observed through a scanning electron microscope (SEM, SH 4000M, Hirox, Oradell, NJ, USA). Fine microstructure and phase separation imaging of the PLA/PCL blends was achieved by using a secondary electron detector at 15 kV and applying magnifications up to x10K.

3. Results and Discussion

3.1. Tensile Testing Analysis

Four formulations of PLA/PCL blends, labeled as shown in Table 1 (95PLA/5PCL, 70PLA/30PCL, 60PLA/40PCL, and 30PLA/70PCL, according to the percentage content of PCL in the PLA matrix), and the pure polymers used as references were subjected to detailed mechanical characterization through tensile experiments.

Receiving of smooth and uninterrupted stress–strain curves allowed for reliable processing of the raw data and proper calculation of the main macromechanical parameters—ultimate strength, Young's modulus, elongation at ultimate strength, and toughness. A plot of the typical stress–strain curves, recorded as a result of successful tensile tests of all specimens at a working velocity of 1 mm/min, can be seen in Figure 1. There should be noticed the steep initial linear part of the σ-ε slopes belonging to the polymer blends with a predominant content of polylactic acid where that elastic regime of stretching reaches the

ultimate tensile stress andunderlines the significant stiffness of the composite materials. The relatively low crosshead motion speed of 1 mm/min and the restricted experimental time of 1000 s may be the reasons that a single fracture point was observed, being registered for the pure PLA. As expected, by adding PCL, the brittleness of the polymer compounds waned, which led to 170% elongation at maximum engineering strain. The increase in the crosshead velocity up to 5 mm/min reduced the test duration, but at the same time, caused an increase in the detected elongation at ultimate deformation reaching an impressive value of 558% with respect to the neat PCL and the 30PLA/70PCL sample (see Figure 2). Moreover, the absence of material failure because of getting to a maximum displacement of the tensile instrument, already reported for similar blends [13], means even potentially higher strain at break due to the impact of PCL on the ability of the 30PLA/70PCL polymer composition to undergo such plastic deformation. The apparent presence of an elastic–plastic mechanical response of all specimens, as evidenced by the formation of necking in the dog-bone work section [21] and reflected in the shape of the curves regardless of the applied crosshead velocity, should be mentioned. The stress–strain curves of the 70PLA/30PCL and 60PLA/40PCL samples imply for a comparable mechanical behavior though the obtained lower yield stress of the blend 70PLA/30PCL at working velocity of 5 mm/min and higher fracture strain of the sample in question at working velocity of 10 mm/min (Figure 3). The reason for this slightly unexpected mechanical data may lie in the microstructural features of both polymer blends, which were examined further by SEM analysis, or in the presence of a tiny defect in the pre-shaped dog-bone specimen that formed upon detachment from the metallic mold.

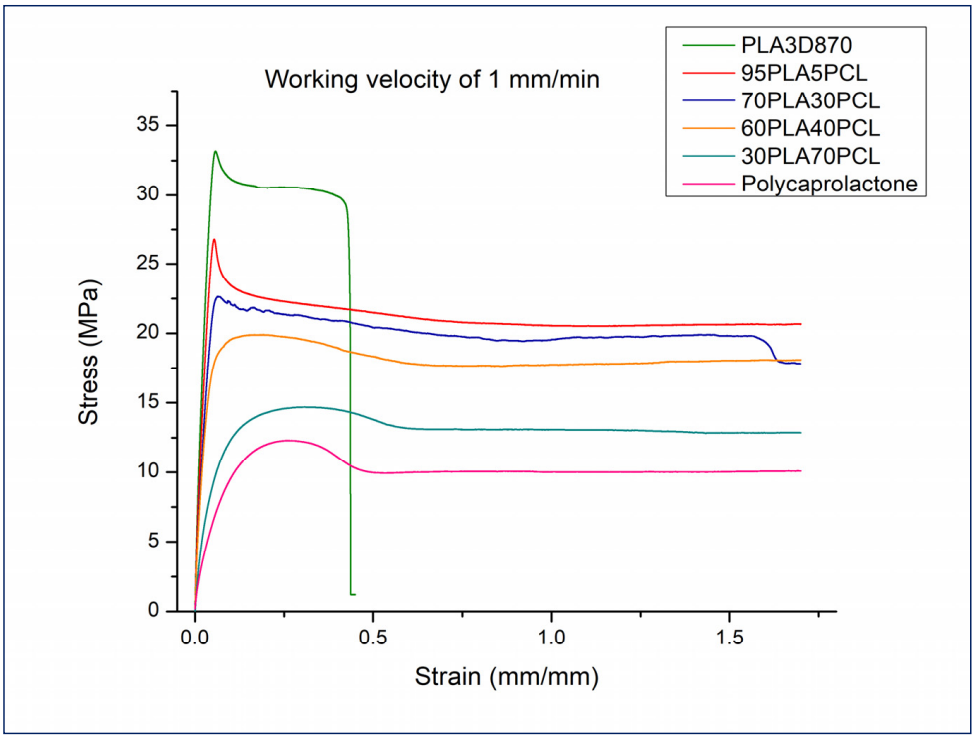

Figure 1. Stress–strain curves of PLA/PCL compositions, including the neat polymers from tensile experiments performed at a working velocity of 1 mm/min.

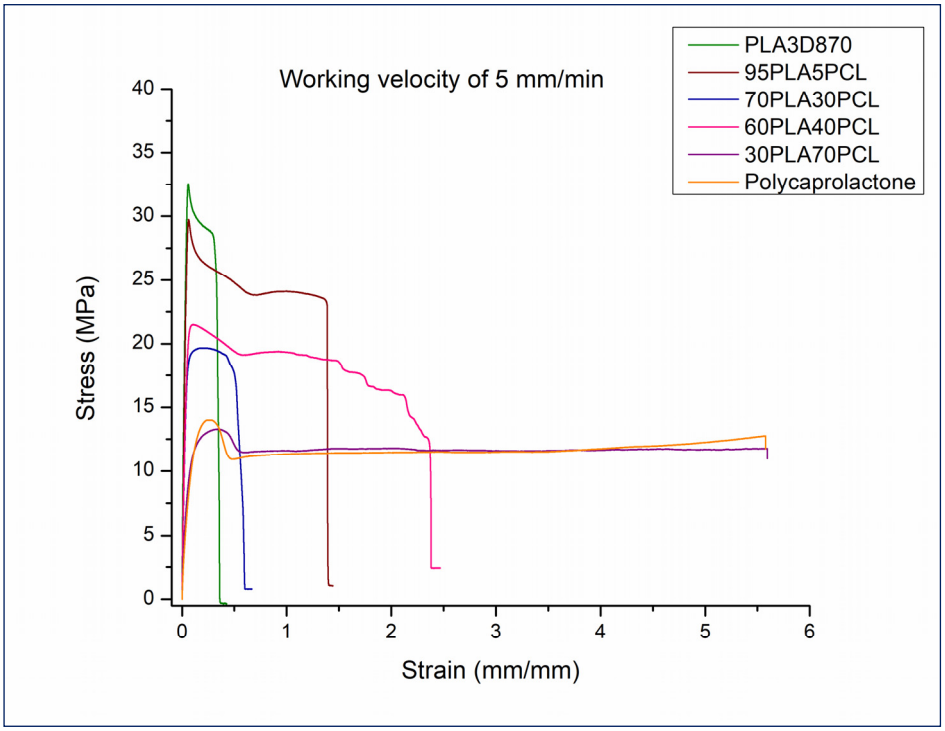

Figure 2. Stress-strain curves of PLA/PCL compositions including the neat polymers from tensile experiments performed at working velocity of 5 mm/min.

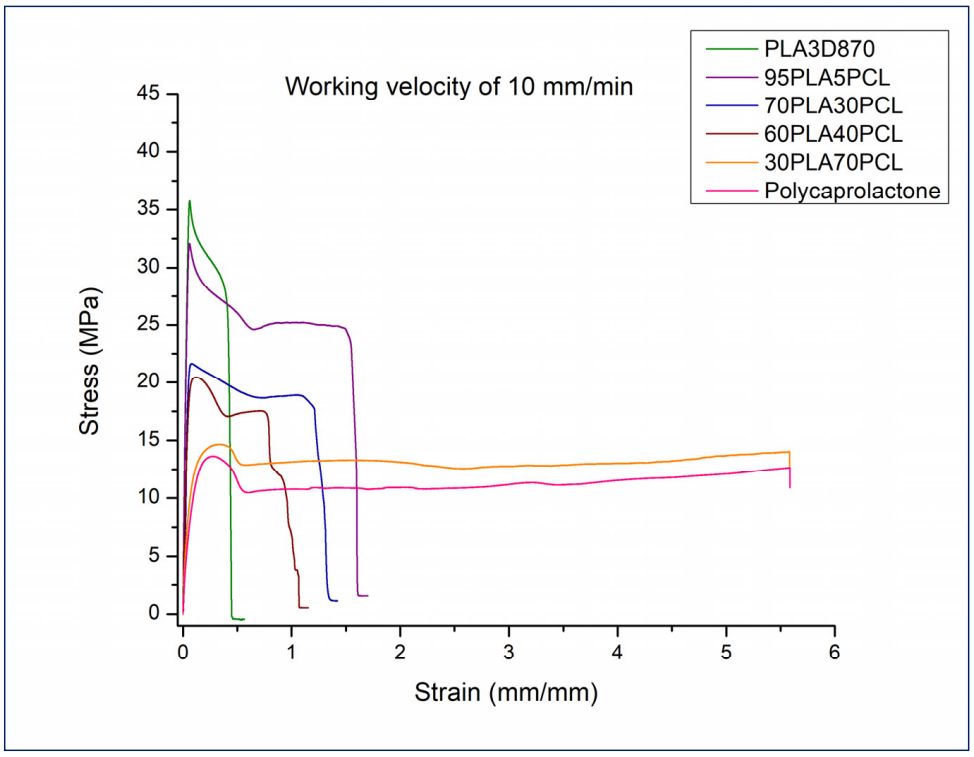

Figure 3. Stress–strain curves of PLA/PCL compositions, including the neat polymers from tensile experiments performed at a working velocity of 10 mm/min.

Generally, the ultimate tensile stress, established by the plotted σ-ε slopes at all applied crosshead velocities, followed the rise of the PLA content in the polymer composites, prompting for a homogeneous dispersion of the PCL particles within the PLA matrix. The enhancement of the tensile working velocity to 10 mm/min did not impede the 30PLA/70PCL blend to come up once again to the limit of crosshead motion, corresponding

to an elongational strain of about 550% and indicating the exceptional ductile properties of that composition. The ultimate tensile strength of the polymer blends as a function of the percentage content of each fraction is presented in Figure 4.

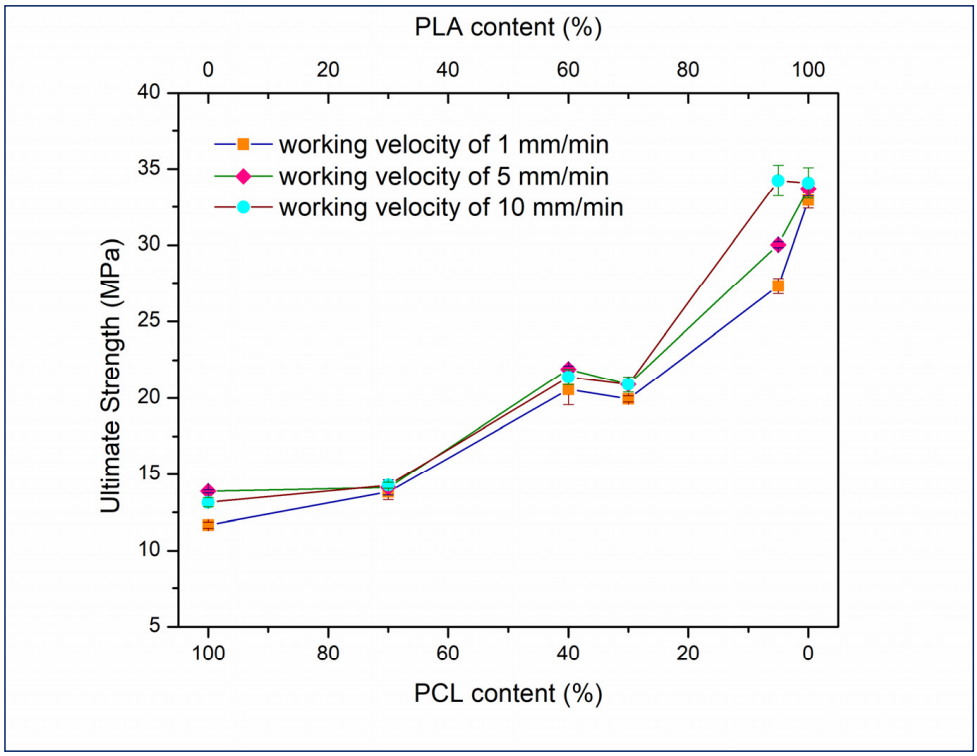

Figure 4. Values of ultimate tensile strength of the polymer compositions at working velocities of 1, 5, and 10 mm/min.

As anticipated, the direction of the maximum strength values goes up with the boosting influence of the PLA weight percentage. However, at a tensile motion of 10 mm/min, the 95PLA/5PCL sample reached almost 35 MPa of ultimate strength, which was slightly above that of the neat PLA. This could be a hint of appearance of a synergistic effect in the mechanical performance of the polymer system, as already described in another study on PLA/PCL blends with optimized composition, processing, and morphology [22]. Regarding the 95PLA/5PCL sample, the dependence of the ultimate tensile stress on the test working velocity, which can be related to the specific morphology of that blend, should be also pointed out. Similar mechanical behavior was noted with respect to the stiffness of the polymer composites having higher PLA content (see Figure 5). Unlike the 95PLA/5PCL and 60PLA/40PCL blends, the 70PLA/30PCL sample demonstrated the best Young's modulus of 438 MPa at the lowest crosshead motion speed of 1 mm/min that can be either due to the microstructural features of the composite material. Interestingly, up to 30 wt% PLA in the specimens, no change was observed in the ultimate tensile strength or in the elastic properties of the 30PLA/70PCL polymer blend. The inclusion of PCL assigned a fully opposite tendency in the slopes depicting the elongation at ultimate strength and the toughness of the composite blends (see Figures 6 and 7). Sensitively higher degree of elongation at maximum tensile stress, surpassing 30%, is visible with regard to the specimen containing 70 wt% PCL. Regarding the 60PLA/40PCL polymer blend, the value calculated at a working velocity of 1 mm/min is an indication that a slower and fine crosshead motion would be beneficial in terms of molecular chain slippages of the polymer phases, resulting in an improvement of the material's elongation up to ultimate strength. In general, there was no obvious difference in the elastic–plastic behavior of the 60PLA/40PCL compound, especially at greater working velocities.

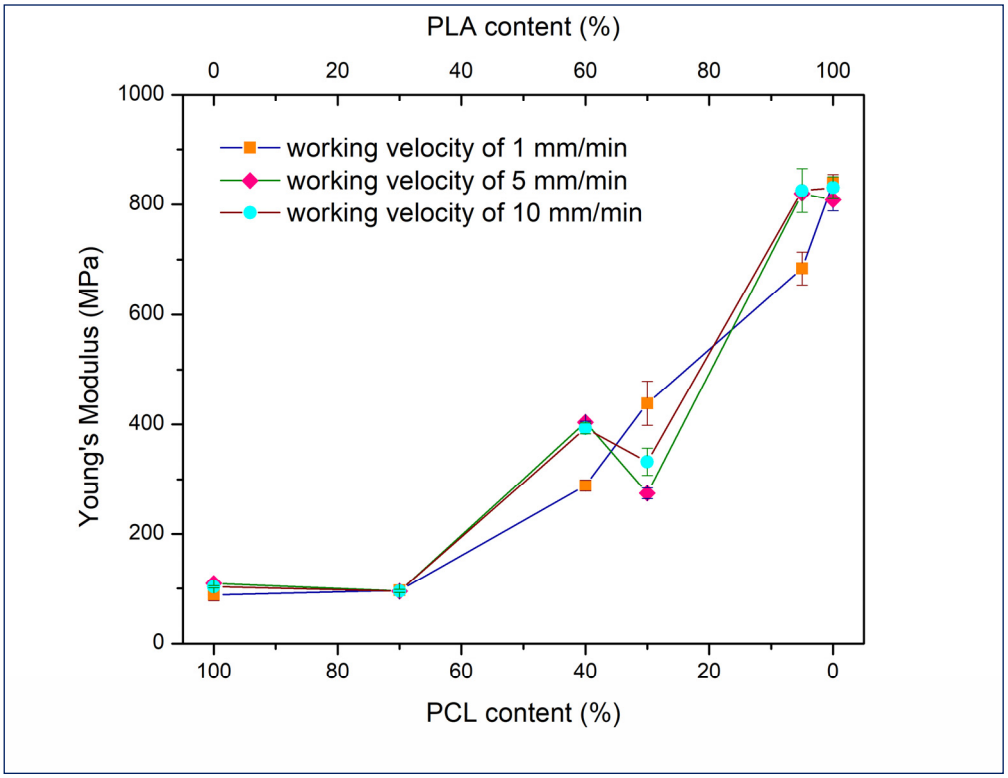

Figure 5. Values of Young's modulus of the polymer compositions at working velocities of 1, 5, and 10 mm/min.

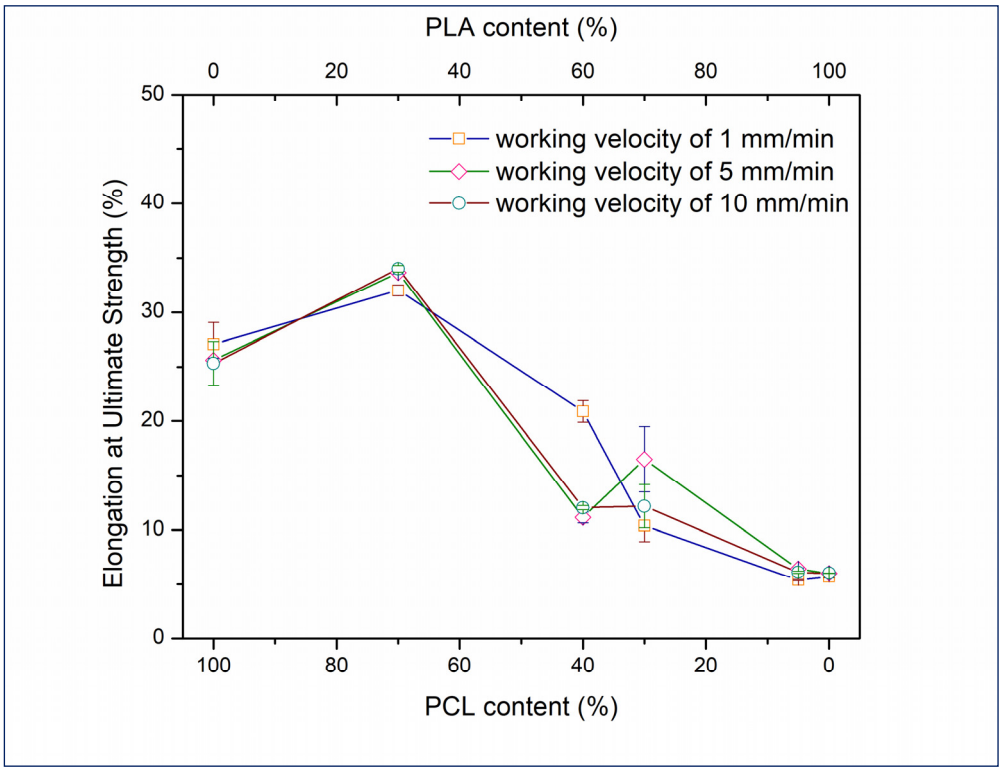

Figure 6. Elongation at ultimate tensile strength of the polymer compositions at working velocities of 1, 5, and 10 mm/min.

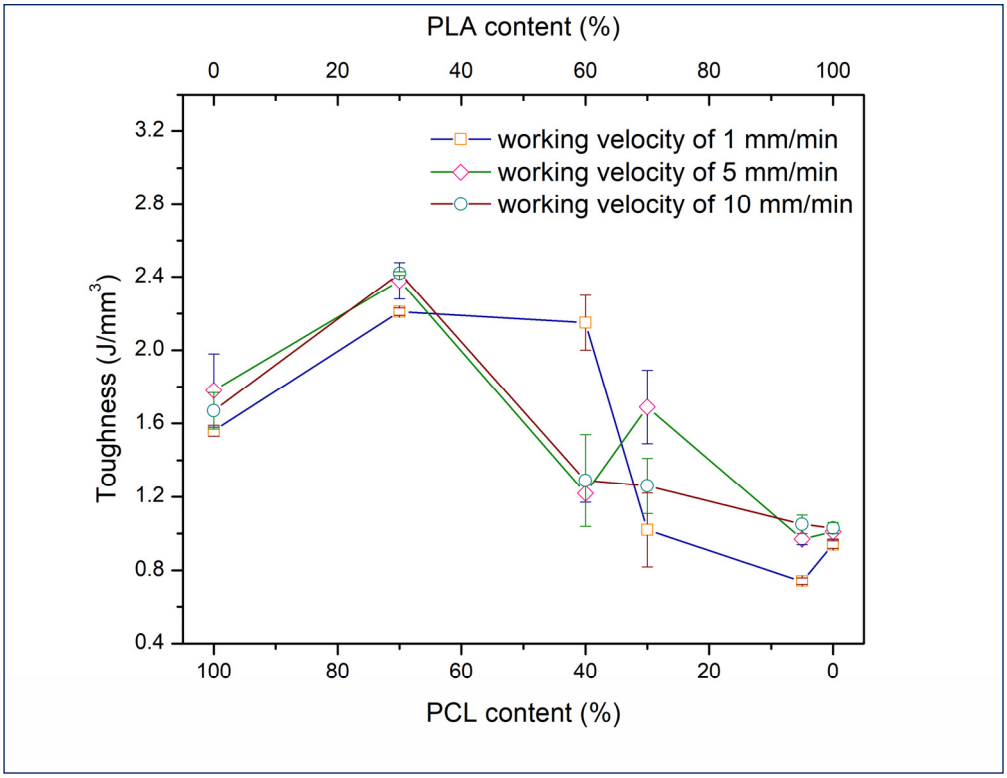

Figure 7. Toughness of the polymer compositions at working velocities of 1, 5, and 10 mm/min.

Despite the present perceptions that the toughness of polymer blends is mostly being evaluated by either impact testing or tensile testing methods, research papers focusing on toughness estimation of PLA/PCL compositions by tensile experiments are rather an exception. Looking at the toughness of the 60PLA/40PCL polymer blend at a crosshead motion speed of 1 mm/min, there can be noticed approximately twice the strain energy absorbed per unit volume up to fracture compared to that of the neat PLA. This is in accordance with the literature data for PLA/PCL blends possessing a close ratio of polymer components and crystallinity similar to the PLA matrix [12,23]. The plasticizing effect of PCL in polymer blends is responsible for the decrease in brittleness of the materials, contributing simultaneously to an enhancement in the ductility of the samples. The registered toughness of the 30PLA/70PCL composition was nearly 2.4 J/mm^3 regardless of the working velocity. As previously mentioned, another relatively high toughness value of 2.15 J/mm^3 standing above the toughness of the pure PCL, was detected with respect to the 60PLA/40PCL composite specimen. The observed impact of the set crosshead motion speed on the stiffness, elongation at ultimate tensile stress, and plastic behavior of the 70PLA/30PCL polymer blend may be attributed to the presence of co-continuous phase morphology, as confirmed by the SEM images shown later in this paper. Summarizing the processed tensile testing data, it should be noted that the selected polymer compositions (70PLA/30PCL, 60PLA/40PCL, and 30PLA/70PCL) demonstrated well-balanced mechanical behavior, especially in terms of ultimate strength, elongation strain, and toughness.

3.2. Shape Memory Characterization of PLA/PCL Strips

Precise estimation of the thermoresponsive shape memory effect of the four PLA/PCL polymer blends was performed in bending mode [24,25] according to the thermomechanical procedure described above in the Materials and Methods section. Figure 8 illustrates the resulting samples' temporary and recovery shapes in the course of the experimental heating–cooling process, including an applied strain over the initial permanent state.

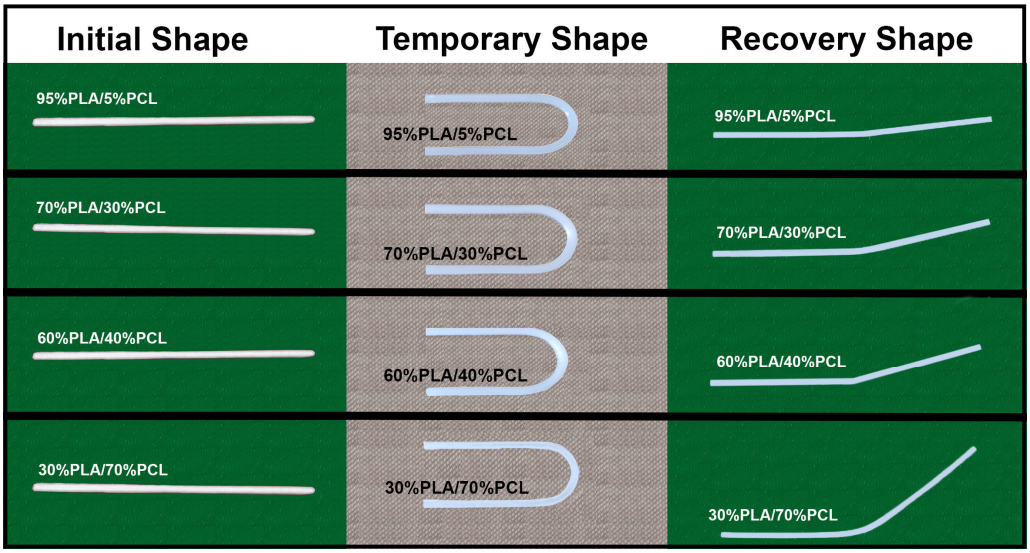

Figure 8. Optical images of the main states describing the shape memory behavior of the PLA/PCL compositions.

All acquired pictures of the treated polymer strips revealed an excellent degree of fixation of the temporary geometry and a very high degree of recovery of the initial geometry in the last testing step, the latter apparently depending on the PLA mass fraction. Measuring both the fixation and recovery angles θ_1 and θ_2 using ImageJ software allowed for the calculation of the R_f and R_r values using Equations (1) and (2). The received indices of shape fixity and shape recovery quantified the capacity of the biopolymer blends to fixate the temporary deformation and to restore the original permanent shape. High shape fixity ratios, near 98%, were found with respect to all investigated PLA/PCL compositions (see Figure 9). This fact could mean a presence of a certain number of unlocked during bending polymer chains whose orientation depends on the crystallization and cross-linking in the cooling step [26]. It may be suggested that at the 60 °C bending temperature, the occurred steering refers to the PCL chains [4], pointing out their importance in the achievement of a significant shape fixation index. Another factor having an impact on the shape fixation rate was the elastic modulus of PLA as the hard segment in the polymer composite material, which was determined to possess exceptional strength–stiffness properties, as shown in the tensile testing section.

When analyzing the shape recovery rate, the role of the polylactic acid cannot be overlooked, as the R_r ratio was found to slightly increase with the rising PLA content in the polymer blend (Figure 9). Generally, the estimated shape recovery indices of the PLA/PCL compositions, measured at 60 °C, ranged between 78.5% and 92.4% (Table 2).

Table 2. Bending shape memory indices of PLA/PCL blends prepared by melt extrusion.

Polymer Blend	R_f [%]	R_r [%] at 60 °C	R_r [%] at 70 °C	R_s [s] at 60 °C	R_s [s] at 70 °C
95PLA/5PCL	96.7	92.4	96.0	70	7
70PLA/30PCL	97.8	91.2	92.7	70	7
60PLA/40PCL	98.3	79.5	82.2	70	7
30PLA/70PCL	97.2	78.5	79.2	70	7

It seems that the higher recovery rate of the samples in which PLA was the main polymer phase may be a function of its continuous nature in the blend microstructure, as depicted below in the SEM analysis section. PLA is likely responsible for hauling, as a hard segment, of much significant recovery stress and serves as driving force to return the strip

in initial shape [19]. Another aspect of the dominant mass fraction of PLA is the effect of its amorphous region as a basic reversible phase having a higher stiffness and therefore a higher resilience than the PCL fraction [16]. To perform an additional experimental approach, a shifting of the recovery temperature up to 70 °C uncovered a distinct shape memory behavior of the PLA/PCL blends in terms of a slightly higher recovery rate (R_r) and mostly concerning the detection of a much shorter shape recovery time (R_s) (see Table 2). As expected, being above the T_m of the PCL resulted in a boosted moving capacity of the PCL molecular chains and, at the same time, probably led to some reduction in the negative effect of both PCL chain slippages and PCL irreversible plastic deformation on the shape recovery index. Most remarkable shape recovery rate at 70 °C was established for the sample 95PLA5PCL, which is in compliance with the already discussed input of PLA as a continuous composite phase in the enhancement of shape recovery capability. It should be mentioned that a really sensitive decrease in the shape recovery time from 70 s at 60 °C to 7 s at θ70 °C was observed in all tested samples. This particular shape recovery behavior could turn out to have great significance for future investigations related to potential smart applications of biopolymer composite materials.

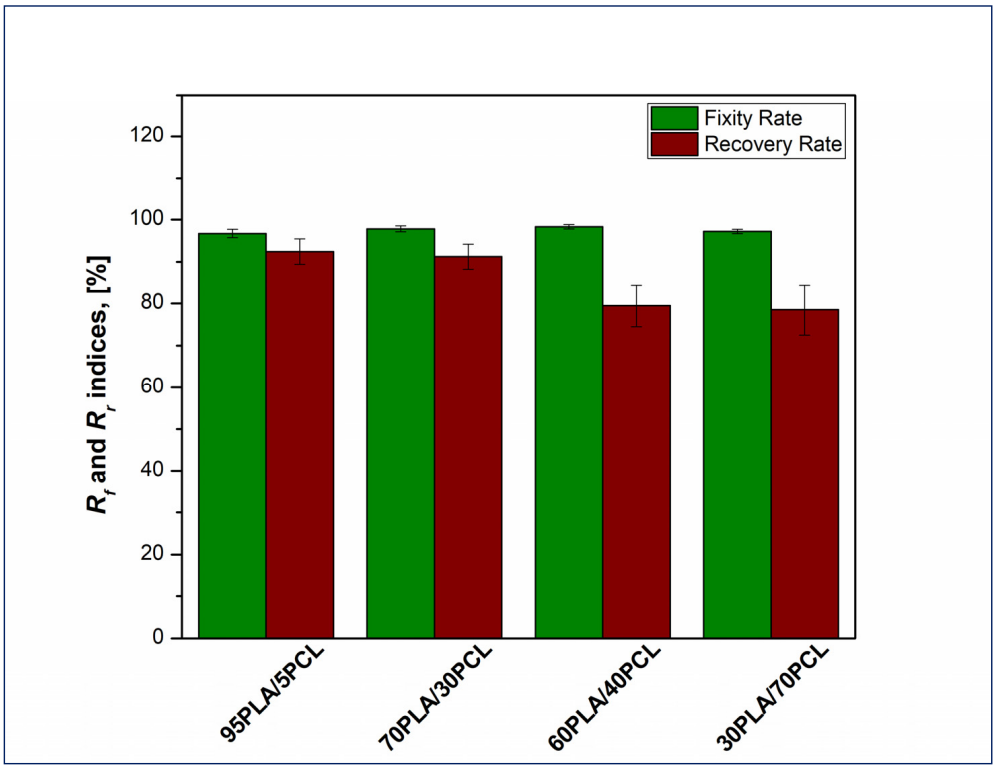

Figure 9. Shape fixation and shape recovery rate evaluation of PLA/PCL composite blends.

3.3. SEM Analysis of PLA/PCL Blends

Scanning electron microscopy images, unveiling the specific morphology of the four polymer blends, are presented in Figure 10.

A formation of a typical round-shaped droplets-in-matrix microstructure [27] can be seen with regard to the cross-section surfaces of the 95PLA/5PCL, 60PLA/40PCL, and 30PLA/70PCL composite samples, while the 70PLA/30PCL polymer blend exhibited a distinct co-continuous phase morphology. The presence of a fine sea-island structure is in a tight connection with the good adhesion between both polymer phases and has a noticeable influence on the toughening of a PLA/PCL blend [28]. Apparently, the tailored composition of the samples, responding to the already established mechanical and shape memory properties, underwent a transition from the porous microstructure of the 95PLA/5PCL

specimen, through the co-continuous morphology of the 70PLA/30PCL blend, and ending with a more compact phase architecture of the polymer composites wherein the PCL content goes up. The conversion of the prevailing polymer phase, playing the role of a matrix, did not change the uniform distribution of the spherical particles belonging to the minor polymer phase, whose size was found to be ~500 nm (see Figure 10a,d). That homogeneous dispersion of polymer droplets, together with the browsed morphological transition, may explain the rise in elongational strain and toughness of the composite samples with increment of the PCL content. The evident immiscibility of the polymer phases did not interfere the occurring of interfacial tension [29], even in the absence of a compatibilizer. This implies that an achievement of optimal composite morphology (~0.5 μm droplet size) can be done by applying appropriate processing conditions, resulting in satisfying mechanical performance of the blends [12,22]. Another indication of possible phase adhesion is the micrograph of the 60PLA/40PCL composition, that is comprised of spherical PCL inclusions showing some extent of deformation when located in a continuous PLA matrix. As illustrated in Figure 10a–d, the narrow bonding of the polymer globular particles in the changing matrix approved the interfacial behavior of the PLA and PCL phases, assisting that way in the transfer of shear stress at the interface and boosting the strength–stiffness properties of the composite specimens.

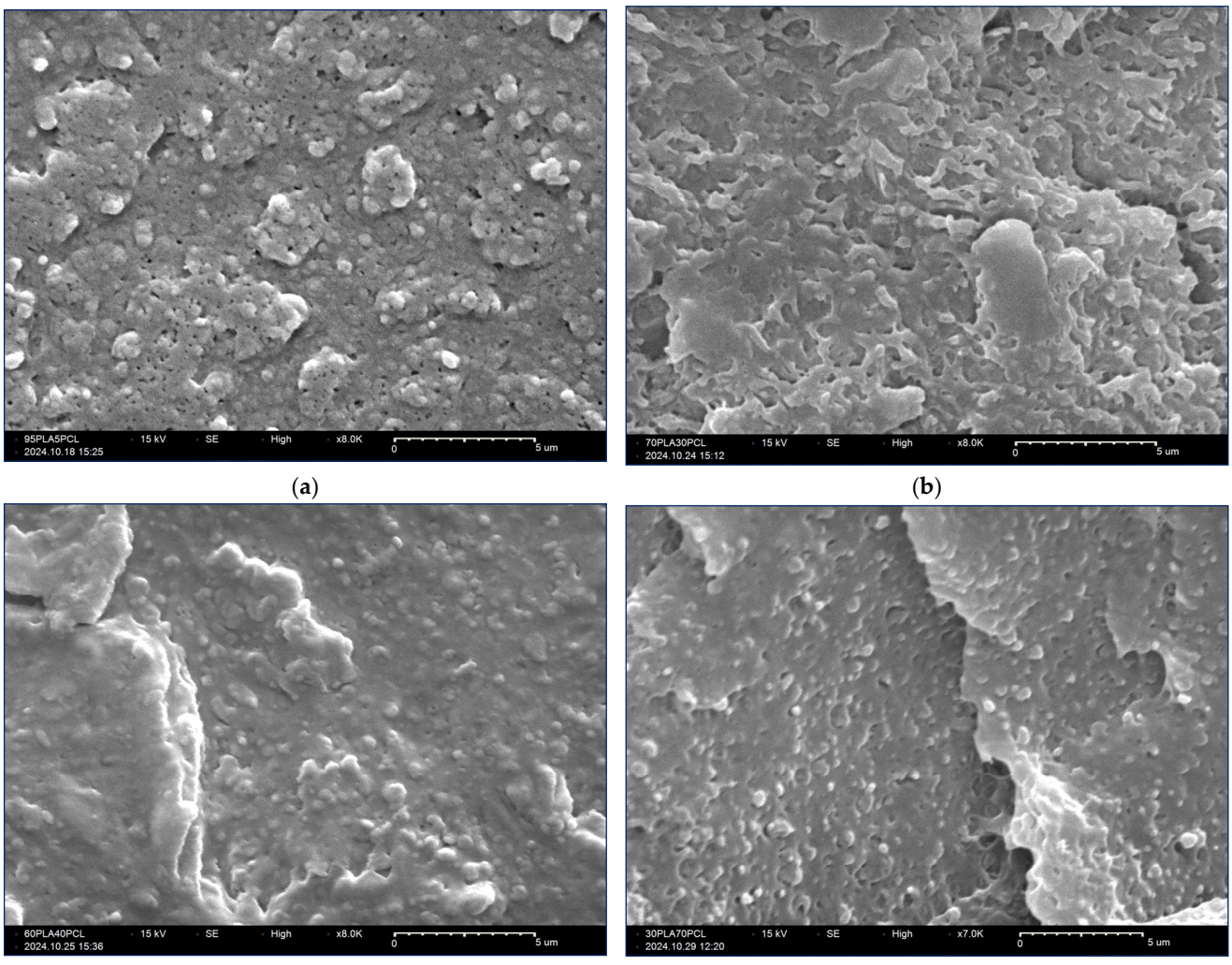

Figure 10. SEM images of cryofractured cross-section surfaces of the melt-extruded polymer blends: 95PLA/5PCL (**a**), 70PLA/30PCL (**b**), 60PLA/40PCL (**c**), and 30PLA/70PCL (**d**).

4. Conclusions

Performing deep mechanical characterization of PLA/PCL blends with tailored compositions testified the adequacy of the preparation method and disclosed the specific function of each one polymer phase with respect to the stiffness and flexibility of the entire composite system. Setting of various crosshead velocities in the tensile script helped in the detailed exploration of the polymer samples to resist elastic and plastic deformation. The objective to design biopolymer composite materials with outstanding mechanical behavior was headed to the subsequent quantification of the shape memory parameters whereof the shape recovery index was found to be highly sensitive towards the degree of PLA content in the blend. The discovered impact of the shape recovery time on the water bath temperature, used to return the polymer strip to its initial shape, may play an important role in future applications of the PLA/PCL compositions. An attentive SEM analysis of the PLA/PCL blends approved their immiscibility and revealed the matter of polymer droplet size in the obtaining of composite materials with remarkable macromechanical and shape memory capacities. The presence of an optimized sample microstructure turned out to be necessary condition to leverage the properties of the individual polymer phases, leading to synergistic improvement in terms of toughness and flexibility of the PLA/PCL blends. The current study aimed to expand the tether with regard to biopolymer composite materials possessing complex mechanical and thermoresponsive shape memory behavior.

Author Contributions: Conceptualization, T.B. and R.K.; methodology, T.B., V.G. and V.A.; validation, T.B., V.G. and E.I.; formal analysis, T.B.; investigation, T.B. and V.G.; resources, E.I., R.K. and V.A.; data curation, V.G. and E.I.; writing—original draft preparation, T.B.; writing—review and editing, T.B. and E.I.; visualization, T.B.; supervision, E.I.; project administration, R.K.; funding acquisition, R.K. All authors have read and agreed to the published version of the manuscript.

Funding: This study was carried out with financial support from the European Union—Next GenerationEU, within Project No. BG-RRP-2.011-0001-C01.

Data Availability Statement: All raw data that underlying the results presented in this study can be provided by the corresponding author upon request.

Conflicts of Interest: The authors declare no conflicts of interest.

References

1. Yusoff, R.B.; Takagi, H.; Nakagaito, A.N. Tensile and flexural properties of polylactic acid-based hybrid green composites reinforced by kenaf, bamboo and coir fibers. *React. Funct. Polym.* **2016**, *94*, 562–573. [CrossRef]
2. Navarro-Baena, I.; Sessini, V.; Dominici, F.; Torre, L.; Kenny, J.M.; Peponi, L. Design of biodegradable blends based on PLA and PCL: From morphological, thermal and mechanical studies to shape memory behavior. *Polym. Degrad. Stab.* **2016**, *132*, 97–108. [CrossRef]
3. Ye, G.; Gu, T.; Chen, B.; Bi, H.; Hu, Y. Mechanical, thermal properties and shape memory behaviors of PLA/PCL/PLA-g-GMA blends. *Polym. Eng. Sci.* **2023**, *63*, 2084–2092. [CrossRef]
4. Molavi, F.K.; Ghasemi, I.; Messori, M.; Esfandeh, M. Nanocomposites based on poly(L-lactide)/poly(ε-caprolactone) blends with triple-shape memory behavior: Effect of the incorporation of graphene nanoplatelets (GNps). *Compos. Sci. Technol.* **2017**, *151*, 219–227. [CrossRef]
5. Kumar, R.; Singh, R.; Kumar, V.; Ranjan, N.; Gupta, J.; Bhura, N. On 3D printed thermoresponsive PCL-PLA nanofibers based architected smart nanoporous scaffolds for tissue reconstruction. *J. Manuf. Process.* **2024**, *119*, 666–681. [CrossRef]
6. Nakajima, H.; Dijkstra, P.; Loos, K. The recent development in biobased polymers toward general and engineering applications; polymers that are upgraded from biodegradable polymers, analogous to petroleum-derived polymers, and newly developed. *Polymers* **2017**, *9*, 523. [CrossRef]
7. Ghafouri, S.E.; Mousavi, S.R.; Khakestani, M.; Mozaffari, S.; Ajami, N.; Khonakdar, H.A. Electrospun nanofibers of poly (lactic acid)/poly (ε-caprolactone) blend for the controlled release of levetiraceta. *Polym. Eng. Sci.* **2022**, *62*, 4070. [CrossRef]
8. Tatu, R.R.; Oria, M.; Rao, M.B.; Peiro, J.L.; Chia-Ying, L. Biodegradation of poly(L-lactic acid) and poly(ε-caprolactone) patches by human amniotic fluid in an in- vitro simulated fetal environment. *Sci. Rep.* **2022**, *12*, 3950. [CrossRef]

9. Molina, B.G.; Ocón, G.; Silva, F.M.; Iribarren, J.I.; Armelin, E.; Alemán, C. Thermally-induced shape memory behavior of polylactic acid/polycaprolactone blends. *Eur. Polym. J.* **2023**, *196*, 112230. [CrossRef]
10. Krishnan, S.; Pandey, P.; Mohanty, S.; Nayak, S.K. Toughening of polylactic acid: An overview of research progress. *Polym.-Plast. Technol. Eng.* **2016**, *55*, 1623–1652. [CrossRef]
11. Fortelny, I.; Ujcic, A.; Fambri, L.; Slouf, M. Phase Structure, Compatibility, and Toughness of PLA/PCL Blends: A Review. *Front. Mater.* **2019**, *6*, 206. [CrossRef]
12. Urquijo, J.; Guerrica-Echavarria, G.; Eguiazabal, J.I. Melt processed PLA/PCL blends: Effect of processing method on phase structure, morphology, and mechanical properties. *J. Appl. Polym. Sci.* **2015**, *132*, 42641. [CrossRef]
13. Simões, C.L.; Viana, J.C.; Cunha, A.M. Mechanical Properties of Poly(ε-caprolactone) and Poly(lactic acid) Blends. *J. Appl. Polym. Sci.* **2009**, *112*, 345–352. [CrossRef]
14. Huang, L.; Sheng, Y.; Mo, Q.; Zhang, S.; Zheng, Y.; Wang, B.; Huang, C.; Duan, Q.; Zhao, H. Poly(lactic acid)/polycaprolactone-based self-programmed photothermal responsive shape memory polymers. *React. Funct. Polym.* **2024**, *202*, 105990. [CrossRef]
15. Wang, Y.; Wang, Y.; Wei, Q.; Zhang, J.; Lei, M.; Li, M.; Li, D. Effects of the composition ratio on the properties of PCL/PLA blends: A kind of thermo-sensitive shape memory polymer composites. *J. Polym. Res.* **2021**, *28*, 451. [CrossRef]
16. Yang, Z.; Yang, Z.; Zeng, J.; Yang, J.; Cao, X. Preparation and Properties of Biodegradable Shape Memory Polylactic Acid/Poly(ε-caprolactone) Blends under Volume Elongational Deformation. *Macromol. Mater. Eng.* **2023**, *308*, 2200342. [CrossRef]
17. Li, A.; Chen, X.-G.; Zhang, L.-Y.; Zhang, Y.-F. Temperature and Infill Density Effects on Thermal, Mechanical and Shape Memory Properties of Polylactic Acid/Poly(ε-caprolactone) Blends for 4D Printing. *Materials* **2022**, *15*, 8838. [CrossRef] [PubMed]
18. Liu, H.; He, H.; Huang, B. Favorable Thermoresponsive Shape Memory Effects of 3D Printed Poly(Lactic Acid)/Poly(epsilon-Caprolactone) Blends Fabricated by Fused Deposition Modeling. *Macromol. Mater. Eng.* **2020**, *305*, 2000295. [CrossRef]
19. Zhou, H.; Xia, Y.; Mu, G.; Gao, Y.; Liang, S.; Li, G.; Yang, Q.; Lin, X.; Qian, F. The preparation and characterization of biodegradable PCL/PLA shape memory blends. *J. Macromol. Sci. Part A Pure Appl. Chem.* **2021**, *58*, 669–676. [CrossRef]
20. Lai, S.M.; Wu, S.H.; Lin, G.G.; Don, T.M. Unusual mechanical properties of melt blended poly(lactic acid) (PLA)/clay nanocomposites. *Euro. Polym. J.* **2014**, *52*, 193–206. [CrossRef]
21. Ivanov, E.; Kotsilkova, R.; Georgiev, V.; Batakliev, T.; Angelov, V. Advanced Rheological, Dynamic Mechanical and Thermal Characterization of Phase-Separation Behavior of PLA/PCL Blends. *J. Manuf. Mater. Process.* **2025**, *9*, 35. [CrossRef]
22. Ostafinska, A.; Fortelny, I.; Nevoralova, M.; Hodan, J.; Kredatusova, J.; Slouf, M. Synergistic effects in mechanical properties of PLA/PCL blends with optimized composition, processing, and morphology. *RSC Adv.* **2015**, *5*, 98971–98982. [CrossRef]
23. Ostafinska, A.; Fortelny, I.; Hodan, J.; Krejcikova, S.; Nevoralova, M.; Kredatusova, J.; Kruliš, Z.; Kotek, J.; Slouf, M. Strong synergistic effects in PLA/PCL blends: Impact of PLA matrix viscosity. *J. Mech. Behav. Biomed. Mater.* **2017**, *69*, 229–241. [CrossRef]
24. Yan, H.; Li, L.; Shi, X.; Yeh, J.-M.; Wei, Y.; Zhang, P. Conductive Stretchable Shape Memory Elastomers Combining with Electrical Stimulation for Synergistic Osteogenic Differentiation. *Polym. Test.* **2020**, *90*, 106672. [CrossRef]
25. Li, M.; Chen, J.; Shi, M.; Zhang, H.; Ma, P.X.; Guo, B. Electroactive anti-oxidant polyurethane elastomers with shape memory property as non-adherent wound dressing to enhance wound healing. *Chem. Eng. J.* **2019**, *375*, 121999. [CrossRef]
26. Gunes, I.S.; Cao, F.; Jana, S.C. Evaluation of nanoparticulate fillers for development of shape memory polyurethane nanocomposites. *Polymer* **2008**, *49*, 2223–2234. [CrossRef]
27. Aliotta, L.; Gigante, V.; Geerinck, R.; Coltelli, M.-B.; Lazzeri, A. Micromechanical analysis and fracture mechanics of poly(lactic acid) (PLA)/polycaprolactone (PCL) binary blends. *Polym. Test.* **2023**, *121*, 107984. [CrossRef]
28. Bai, H.; Huang, C.; Xiu, H.; Gao, Y.; Zhang, Q.; Fu, Q. Toughening of poly(L-lactide) with poly(epsilon-caprolactone): Combined effects of matrix crystallization and impact modifier particle size. *Polymer* **2013**, *54*, 5257–5266. [CrossRef]
29. Broz, M.E.; VanderHart, D.L.; Washburn, N.R. Structure and mechanical properties of poly(D,L-lactic acid)/poly(ε-caprolactone) blends. *Biomaterials* **2003**, *24*, 4181–4190. [CrossRef]

Disclaimer/Publisher's Note: The statements, opinions and data contained in all publications are solely those of the individual author(s) and contributor(s) and not of MDPI and/or the editor(s). MDPI and/or the editor(s) disclaim responsibility for any injury to people or property resulting from any ideas, methods, instructions or products referred to in the content.